Article

Influence of an Oxygen-Free Atmosphere on Process Forces and Workpiece Quality during the Surface Grinding of Ti-6Al-4V

Berend Denkena, Benjamin Bergmann [ID] **, Nils Hansen and Roman Lang** *[ID]

Institute of Production Engineering and Machine Tools (IFW), Leibniz University Hannover, An der Universität 2, 30823 Garbsen, Germany
* Correspondence: lang@ifw.uni-hannover.de; Tel.: +49-511-762-18223

Abstract: Most manufacturing processes, such as grinding, are usually conducted in a standard air atmosphere. The oxygen within this atmosphere leads to oxidation effects on tools and workpieces when machining metal components. This is primarily a factor in the processing of titanium due to its high affinity for oxygen. The oxidation of the surface increases tool wear and reduces surface quality. Hence, this paper investigates the influence of the atmosphere on process forces and workpiece quality when grinding titanium (Ti6Al4V) with metal-bonded diamond grinding tools. To generate oxygen-free conditions in production processes, a novel approach allows an atmosphere with a very low oxygen partial pressure. Using a silane gas, which reacts with oxygen, the oxygen partial pressure, p_{O2}, can be reduced below 10^{-12} mbar, equal to the oxygen partial pressure in an extremely high vacuum (XHV). The results show a significant influence of the atmosphere on the process forces. When grinding in XHV-adequate conditions, the grinding forces are reduced by 16% in the tangential direction and 50% in the normal direction on average, while the quality of the ground titanium surfaces is consistent (both atmospheres: Rz = 13–21 μm). Phase analysis via XRD revealed a distinct amount of titanium nitride (TiN) on the ground surfaces independently of the atmospheric conditions.

Keywords: surface grinding; oxygen-free atmosphere; titanium; mechanical load; XHV

1. Introduction

Concerning economically efficient manufacturing processes and the quality of machined components, the demands on production technology are constantly increasing. For this reason, manufacturing processes must be continuously developed. In precision machining, the surface quality of components is a critical evaluation parameter. Grinding is the most frequently used finishing process, which enables particularly high surface qualities [1–3].

When grinding difficult-to-machine materials, such as titanium (Ti), tool wear limits economic efficiency by increasing manufacturing costs [4–6]. Oxidation processes, particularly, are expected to play a key role in tool wear when machining titanium due to its high oxygen affinity. Nevertheless, titanium is of particular industrial importance as it is used for structural components in many industries (e.g., aerospace) due to its excellent corrosion resistance, low density, and high strength [7]. The most frequently used alloy in this field is Ti-6Al-4V, which will be the material investigated in this paper [8,9].

Since titanium has a particularly high affinity for oxygen, the material tends to show pronounced oxidation behavior, which can already be observed in a typical air atmosphere and at room temperature. Because of the high process temperatures during grinding, this effect is amplified and leads to a significant hardening and embrittlement of the component surface [10]. This, in turn, results in increased tool wear and reduced surface qualities of the components [4].

In additionally Ti-6Al-4V, base oil as a cutting fluid also has only limited oxidation stability. Especially due to the increased temperatures in the contact gap between the

grinding wheel and the workpiece, oil has increased reactivity to atmospheric oxygen. The oxidative degradation of the oil can lead to a reduction in the tribological properties and thus to increased friction in the process [11].

An entirely new approach to avoiding these oxidation processes is eliminating the oxygen content in the machining atmosphere. This is currently being investigated at the Institute of Production Engineering and Machine Tools within the "Collaborative Research Center 1368 SP C04". In the current study, the influence of the grinding atmosphere on the grinding process and the resulting surface quality will be examined. For this, a surface grinding process was conducted in air and oxygen-free conditions, and the process forces were measured. Subsequently, the workpiece quality was investigated using microscope images, X-ray diffraction, and surface roughness measurements.

2. Materials and Methods

2.1. Oxygen-Free Atmosphere

A standard method to eliminate oxygen from the atmosphere is to remove the molecules from an enclosed space by creating a technical vacuum. Another approach is to replace the oxygen with a second gaseous medium or use a gas that causes a chemical reaction with oxygen. The presented investigations use a combination of these two methods. In the first step, oxygen will be displaced by the heavier and chemically inert argon (Ar). In the second step, a low amount of the gas mixture argon/silane (Ar/SiH$_4$) with 1.5 V% silane is used to reach XHV-adequate oxygen partial pressure. The silane reacts with the oxygen and water residues using the following chemical reactions [12].

$$SiH_4 + 2O_2 \rightarrow SiO_2 + 2H_2O \tag{1}$$

$$SiH_4 + 2H_2O \rightarrow SiO_2 + 4H_2 \tag{2}$$

This reaction chain leads to the formation of hydrogen and silicon dioxide [13]. Using these reactions generates an atmosphere with a very low oxygen partial pressure, p$_{O2}$, of $\leq$10 20 mbar at ambient air pressure [14]. Concerning the oxygen content, the resulting atmosphere is equivalent to an extremely high vacuum (XHV), which starts at 10^{-12} mbar [15]. The advantage of this approach is that it is much less complex than is that of using a conventional technical vacuum.

2.2. Experimental Setup

The experimental grinding investigations were carried out on a Geibel & Hotz FS840 KT CNC (Geibel & Hotz GmbH, Homberg, Germany) surface-grinding machine. Gastight housing has been extended to this to enable tests in XHV conditions (Figure 1). The housing enabled the supply of the gas mixture Ar/SiH$_4$ and cooling lubricant for the actual grinding process. The grinding tool used was a bronze-bonded diamond grinding wheel (80/20 copper/tin, D46, C75) machining Ti-6Al-4V (Ti64) in a surface-grinding process. The grinding wheel was dressed (q$_d$ = $-$0.8, v$_{cd}$ = v$_c$, v$_{fd}$ = 1500 mm/min, a$_{ed}$ = 5 μm) and sharpened (v$_{cs}$ = v$_c$, v$_{fs}$ = 100 mm/min, a$_{es}$ = 100 μm) before every single experiment using a dresser with a #120-SiC wheel and a white corundum sharpening stone with a grain size of #180. To evaluate the mechanical load of the process, the grinding forces were measured with a Kistler 9257B dynamometer (Kistler Instrumente AG, Winterthur, Switzerland).

To create an XHV-adequate atmosphere, gastight housing within the Geibel & Hotz (FS840 KT CNC) surface-grinding machine was used. The gas mixture of Argon/Silane was tapped near the contact zone between the grinding tool and the workpiece (Figure 1, left). To validate the XHV-adequate atmosphere, the oxygen partial pressure was measured with an oxygen sensor and recorded using Raspberry Pi. (Figure 1, right). A preset filter at the sensor prevented oil and SiO$_2$ particles from entering the oxygen sensor. How the XHV-adequate atmosphere was established in detail is shown in chapter 3.1.
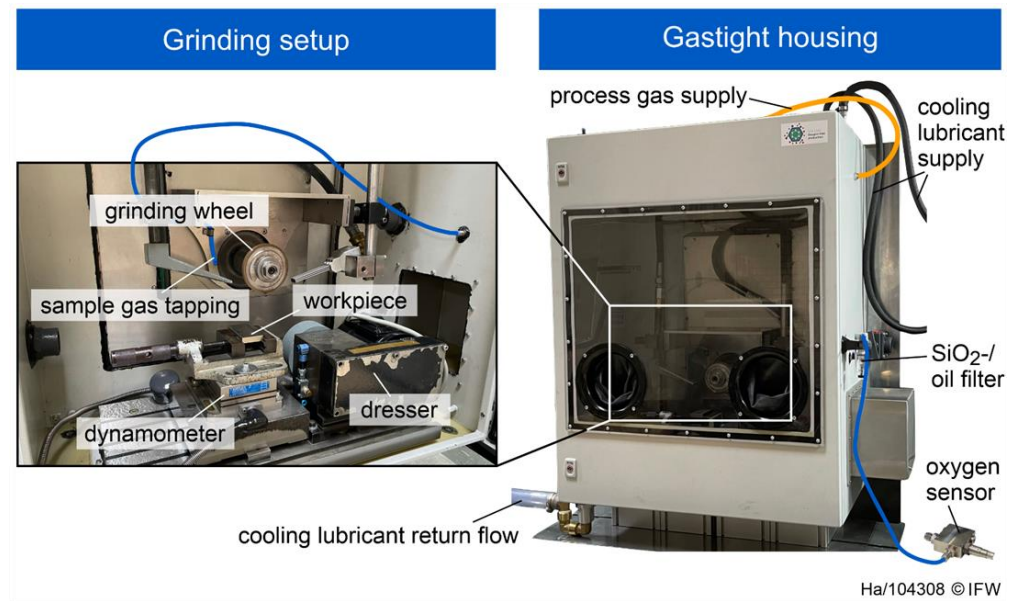
Figure 1. Experimental setup for grinding in an XHV-adequate atmosphere.

2.3. Grinding Process Parameters

The process parameters cutting speed, v_c, and feed rate, v_f, were varied in a reasonable process window during grinding, as shown in Table 1. This enabled the determination of the influence of different atmospheres (air/XHV) on the mechanical load (process forces) and the workpiece surface quality for other loads. The parameter sets were performed for air and the XHV-adequate atmosphere, and each set was repeated twice. This resulted in a total of 30 experiments. The single-grain chip thickness, h_{cu}, was calculated according to the $F_{RIEMUTH}$ to evaluate different loads using the following formula:

$$h_{cu} = \left(\frac{1}{C2+1}\right)^{\frac{1}{C2}} * \left(\frac{C2+1}{C1*N_{GV}} * \frac{Q'_w}{v_c*l_g}\right)^{\frac{1}{C2+1}} \tag{3}$$

$$\text{with } N_{GV} = \frac{6*C}{\pi*\rho_G*d_G^3} \; ; \; C1 = \frac{4}{3}*\sqrt{d_G}; \; C2 = 1.5 \tag{4}$$

where C1 and C2 are parameters for the grain type used in the grinding wheel, and N_{GV} is the number of active cutting edges. C, ρ_G and d_G are the grain concentration, density of the grain and the grain diameter, respectively. Q'_w is the material removal rate and l_g is the geometric contact length between the workpiece and the grinding wheel [16].

Table 1. Processed parameter sets for grinding in air and XHV-adequate atmosphere.

Set	v_c in m/s	v_f in mm/min	h_{cu} in μm
1	12.5	100	0.30
2	12.5	400	0.52
3	18.75	250	0.37
4	25	100	0.23
5	25	400	0.40

2.4. Measurements Methods

The ground specimens were examined using a Keyence VHX-600 (Keyence, Osaka, Japan) reflected light microscope. Furthermore, the roughness parameters of the ground surfaces were measured using a Mahr MarSurf LD 130 tactile measuring device (Mahr GmbH, Göttingen, Germany). The direction of measurement was orthogonal to the direction of the cut, and each surface was measured five times at different positions to ensure

statistical reliability. In addition, the surfaces were examined via XRD phase analysis. These measurements were conducted using a Seifert XRD 3003 TT diffractometer (Richard Seifert & Co, Ahrensburg, Germany) with a cobalt target to detect any phases that might have formed on the titanium surface due to chemical reactions during grinding. All measurements were performed with identical measurement settings and in similar conditions. The measured diffraction patterns were evaluated using PowderCell 2.4 software [17].

3. Results and Discussions

The following section discusses the process conditions regarding the oxygen partial pressure, p_{O2}, before analyzing the process forces during grinding in both atmospheres (air/XHV) and the resulting workpiece surface qualities.

3.1. Process Conditions

Before grinding experiments in the XHV-adequate atmosphere could be carried out, the oxygen had to be removed from the gastight housing. Figure 2 shows an exemplary measurement of the oxygen partial pressure during the process of oxygen removal.
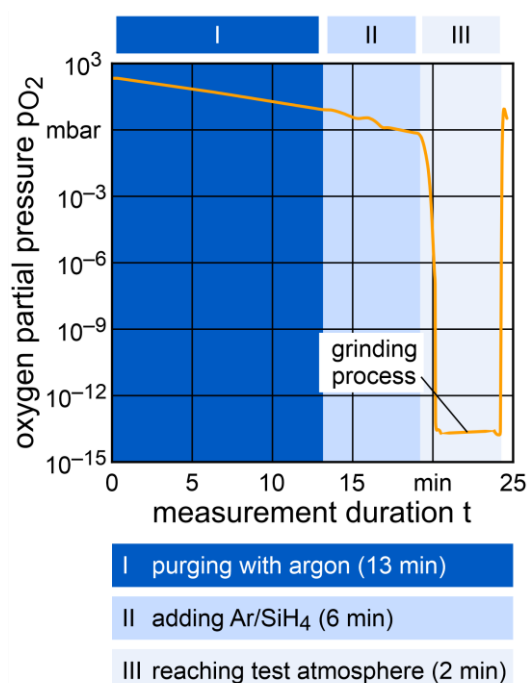

Figure 2. Oxygen measurement during a grinding experiment at a low oxygen partial pressure.

In the first step, purging the housing with argon decreased the oxygen partial pressure, p_{O2}, to about 10 mbar (phase I). The subsequent addition of argon/silane (98.5/1.5 V%) caused the oxygen partial pressure to drop to approximately 10^{-14} mbar within 8 min (phase II + III). The time delay between the introduction of the argon/silane gas mixture and the first measurable oxygen reaction was 6 min and this can be explained by the fact that the positions of the gas introduction and the gas measuring point were relatively far apart (phase II). As soon as an oxygen partial pressure of 10^{-14} mbar (XHV-adequate) was reached, the grinding process was carried out. At the end of the process, the gas was extracted by the vacuum and the door of the housing was opened resulting in the sudden increase in oxygen partial pressure.

Table 2 shows that the grinding processes were always carried out at slightly different oxygen partial pressure levels. The oxygen partial pressure was in a range of $p_{O2} \approx 10^{-14}$ to 10^{-19} mbar since the reaction of oxygen and silane occurs very quickly and the oxygen partial pressure reduction rate is very high. However, all grinding experiments were conducted at XHV-adequate oxygen partial pressure ($p_{O2} \leq 10^{-12}$ mbar).

Table 2. XHV-adequate atmosphere validation through oxygen partial pressure measurements.

Set	p_{O2} in mbar	h_{cu} in µm
1	$6.0 \times 10^{-13} \dots 8.8 \times 10^{-16}$	0.30
2	$1.5 \times 10^{-14} \dots 4.7 \times 10^{-17}$	0.52
3	$7.5 \times 10^{-16} \dots 2.5 \times 10^{-19}$	0.37
4	$4.5 \times 10^{-14} \dots 5.6 \times 10^{-17}$	0.23
5	$8.4 \times 10^{-15} \dots 1.4 \times 10^{-17}$	0.40

3.2. Process Forces

To evaluate the mechanical load during grinding in air and under a low oxygen partial pressure ($p_{O2} < 10^{-13}$ mbar), the process forces in the tangential (F_t) and normal direction (F_n) were measured. In the grinding experiment, the cutting speed, v_c, and the feed rate, v_f, were varied, while the depth of cut was constant at $a_e = 50$ µm. These three process parameters could be combined within the single-grain chip thickness, h_{cu}, which could be interpreted as a physical quantity of the load on the abrasive grains of the grinding tool during machining [16]. The single-grain chip thickness could then be correlated with the grinding forces, as illustrated in Figure 3.
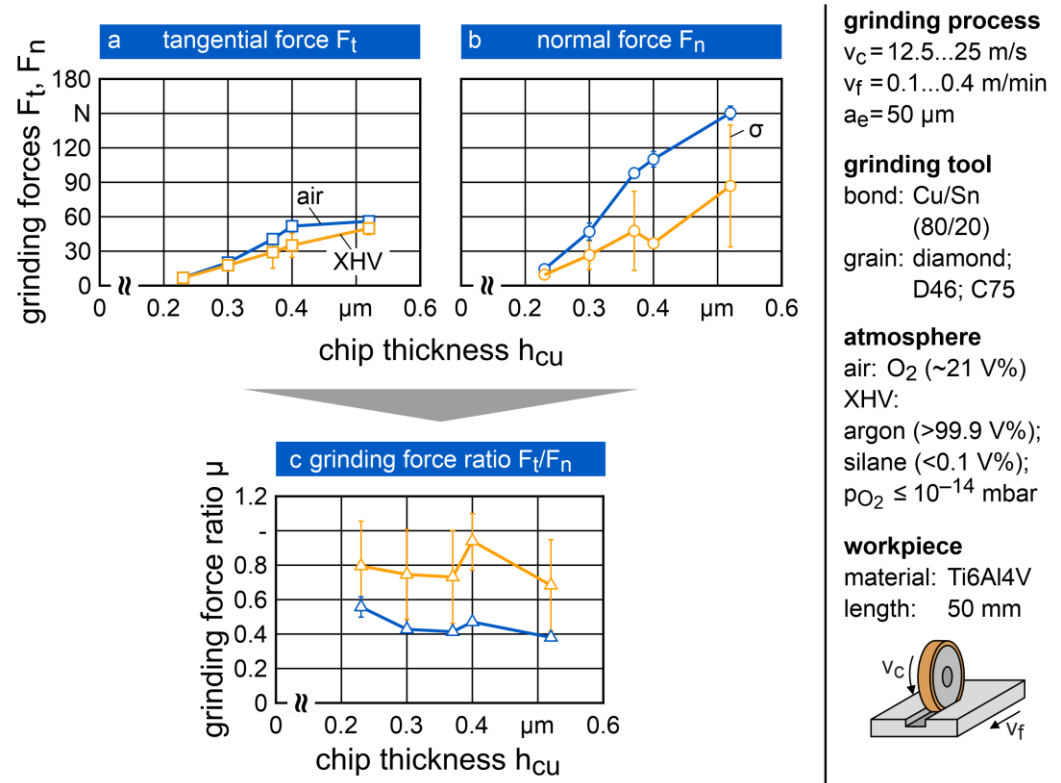

Figure 3. Tangential forces (**a**), normal forces (**b**), and grinding force ratio (**c**) during surface grinding in air and under XHV-adequate atmosphere.

An increasing linear correlation between grinding force directions and chip thickness could be observed. With an increasing single-grain chip thickness, the mechanical load also increased. The main reasons were the decreasing cutting speeds and increasing feed rates that caused a rise in chip thickness, according to $F_{RIEMUTH}$ [16]. The performed experiments showed a significant difference in grinding forces between grinding in air and XHV (Figure 3a,b). The absolute force values during grinding in XHV were 16% (F_t) and 50% (F_n) lower on average.

Consequently, the XHV-adequate atmosphere influenced the grinding process significantly, particularly at higher loads. The reduction in the normal force reached a

maximum at h_{cu} = 0.4 μm. A possible explanation for the reduction in the normal forces, especially at higher loads and therefore higher temperatures within the contact zone, could be the thermal and oxidative degradation of the cutting fluid due to the reaction with oxygen. At elevated temperatures of more than 120 °C, the hydrocarbons within the cutting oil start to degrade in terms of serval products such as aldehydes or ketones [18], sludge [19], or volatile CO_2 [20]. These products have undesirable tribological properties compared to the original cutting fluid and can therefore aggravate the grinding process. Especially, the formation of CO_2 can result in an insufficient lubricant film within the contact zone due to the displacement of the film. If the reaction with oxygen does not occur due the XHV-adequate atmosphere, the oil stability increases at a temperature below boiling point and results in improved application behavior with friction and therefore lower normal forces. The grinding force ratio, μ, is described by the quotient of the tangential and normal force, which represents the ratio of cutting and friction processes. A higher grinding force ratio means the cutting process is more efficient, while a lower ratio represents higher friction in the contact zone, resulting in a less efficient grinding process. Sharper cutting edges lead to a larger grinding force ratio while progressive tool wear causes a decrease in the grinding force ratio [1]. The ratio is expected to increase with increasing chip thickness due to the more pronounced cutting of the material. However, the opposite effect could be observed in the present investigations when grinding in XHV and in air (Figure 3c). This can be explained via observations of chips that adhered to the grinding wheel's surface during grinding. These chips caused the clogging of the chip space of the wheel and thus increased the normal forces. Grinding in the XHV-adequate atmosphere shows significantly higher grinding force ratios than that in air. The force ratio increases by 40% on average due to a higher decrease in the normal forces compared to the tangential forces.

3.3. Workpiece Surface Quality

Microscope images of the ground workpieces were taken to analyze the workpiece surface. In Figure 4, the resulting surfaces of grinding processes in air and XHV for different chip thicknesses, h_{cu}, are compared. An increasing chip thickness changes the surface towards a more pronounced welding-on of titanium chips (workpiece) and of bronze bond (grinding tool). These welding-on effects first appear at h_{cu} = 0.37 μm and intensify with increasing chip thickness. Visible dark surface discoloration starts at h_{cu} = 0.37 μm, indicating a distinct temperature-induced grinding burn. However, these effects are comparable between grinding in air and an XHV.
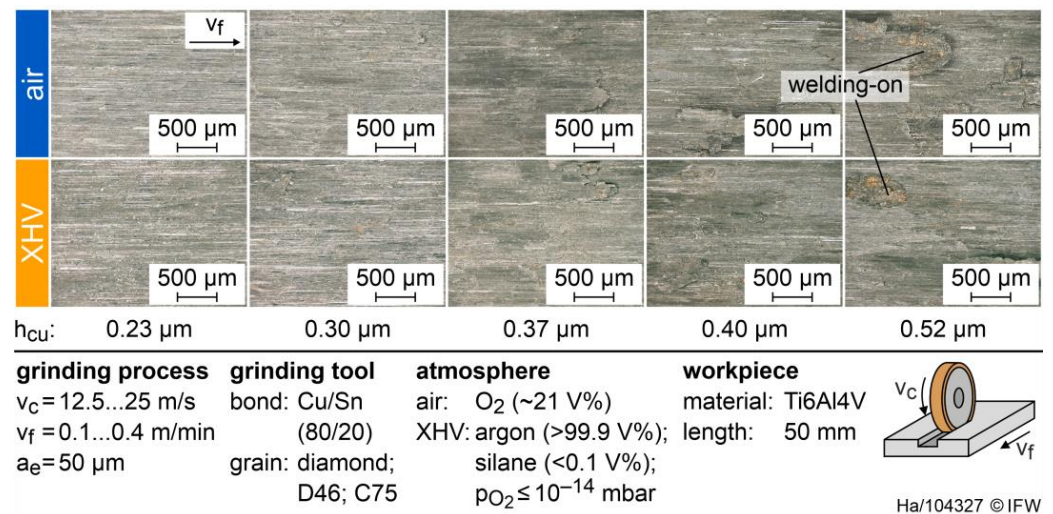

Figure 4. Microscope images of ground Ti64 workpiece surfaces.

In Figure 5, the surface roughness of ground titanium workpieces is shown. The results also support the visual analysis (Figure 4) since no correlation between the grinding atmosphere and the surface roughness (R_z = 13–21 µm) can be found. The main reason is that the influence of the grinding wheel's topography and process parameters is much higher than the influence of the atmosphere. The roughness generated in different atmospheres is nearly congruent. The decreased roughness at h_{cu} = 0.40 µm can be explained by the highest cutting speed of v_c = 25 m/s, which leads to the lowest surface roughness.
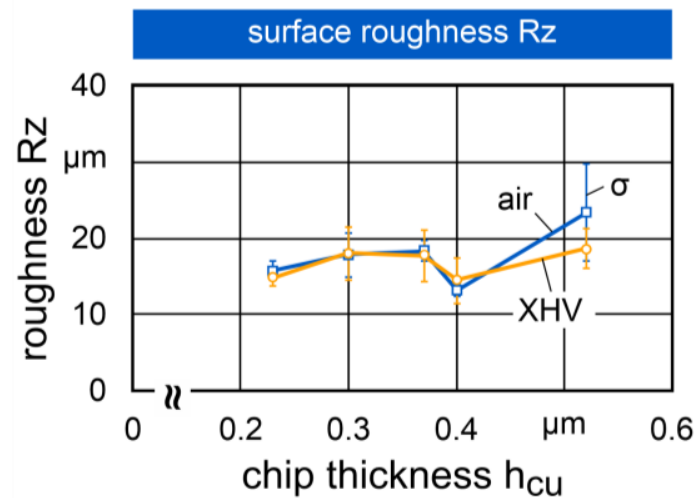
Figure 5. Surface roughness of ground Ti64 workpieces.

To further analyze the titanium surface, an XRD phase analysis was performed. No quantitative differences in peak intensities and positions were found between the different process parameter sets. For this reason, a representative sample that was ground with a chip thickness of h_{cu} = 0.23 µm is shown in Figure 6. The reference measurement of the workpiece before grinding shows that only titanium was present on the surface. After grinding, additional peaks appeared to be identical in position and intensity for the two machining atmospheres (air/XHV). These peaks mainly represent titanium nitride (TiN) formed on the surfaces in both atmospheres [21]. Since only oxygen was removed from the gastight housing, some residual nitrogen content was likely still present in the XHV-adequate atmosphere. During grinding, the nitrogen reacted with the newly formed titanium surface due to the elevated grinding temperatures, resulting in the formation of a titanium nitride layer. An oxide layer could not be detected during grinding since the XRD measurement method is unsuitable for detecting very thin layers.
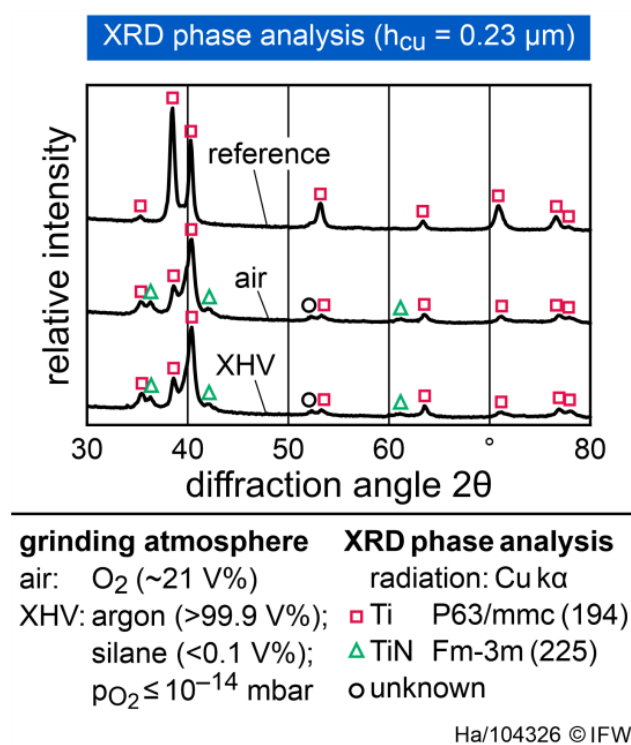
Figure 6. XRD phase analysis of ground Ti64 workpieces.

4. Conclusions

In conclusion, the findings from this research provide valuable insights into the influence of the grinding atmosphere on the grinding process. The experimental setup successfully achieved conditions equivalent to an extreme high vacuum (XHV) with an oxygen partial pressure (p_{O2}) of $\leq 10^{-12}$ mbar. Grinding in an XHV-adequate atmosphere resulted in a significant reduction in process forces, with average decreases of 16% in the tangential direction and 50% in the normal direction compared to those when grinding in air.

Furthermore, the XHV-adequate atmosphere did not have a significant impact on the quality of the titanium surfaces in terms of visual appearance (grinding burn), surface roughness (R_z = 13–21 µm), and material composition within the investigated range of parameters (v_c = 12.5–25 m/s, v_f = 100–400 mm/min). Both grinding in air and XHV environments led to the formation of a TiN phase on the titanium surfaces, with no detectable oxide layer in either case.

These results highlight the significant influence of oxygen content within the grinding atmosphere on the process forces. Utilizing an XHV-adequate atmosphere has the potential to decrease grinding forces, positively impacting grinding tool life, process efficiency, and energy consumption. Additionally, an absence of oxidative degradation of the cutting fluid in an XHV-adequate atmosphere may improve tribological properties and application behavior. In line with these findings, several hypotheses can be proposed:

- The absence of oxygen prevents the surface from passivating, which alters the microstructure and deformation behavior during chip formation. Future investigations can explore the impact of non-passivated surfaces on chip formation, microstructure evolution, and associated deformation behavior during the grinding process.
- A passivated layer exhibits different surface characteristics from those of a non-passivated layer. As a result, the wetting behavior of the oil on the surface may also change, leading to different cooling and lubricating effects. Investigating the influence of passivation layers on the wetting behavior of the oil and the subsequent cooling and lubricating effects can provide insights into optimizing the grinding process.

- The reaction between silane and residual oxygen results in the formation of amorphous SiO_2 particles. It is possible that these particles are present in the grinding oil and act as friction-reducing agents in the grinding contact. Exploring the presence and role of these amorphous SiO_2 particles in the grinding oil can shed light on their contribution to friction reduction and overall process performance.

This will be the subject of future investigations, in addition to the general wear behavior when grinding in an XHV-adequate atmosphere and the resulting hardness of workpiece surfaces. In addition, future research will focus on investigating the effects of an oxygen-free atmosphere on materials beyond Ti-6Al-4V. Aluminum alloys, steel and cemented carbides also form a thin oxide layer on their surface and are therefore interesting to investigate to reach a deeper understanding of the improvement of the grinding process under an XHV-adequate atmosphere.

Author Contributions: B.D. was responsible for funding acquisition and project administration and reviewed and edited the article together with B.B. in the writing process. B.B. supervised the project. N.H. conducted the experiments, analyzed the data and wrote the manuscript. R.L. analyzed the data, revised and finalized the manuscript. All authors have read and agreed to the published version of the manuscript.

Data Availability Statement: Available on request.

Nomenclature

a_e	Depth of cut in mm
a_{ed}	Depth of cut during dressing in mm
a_{es}	Depth of cut during sharpening in mm
F_n	Normal force in N
F_t	Tangential force in N
h_{cu}	Single-grain chip thickness in μm
p_{O2}	Oxygen partial pressure in mbar
q_d	Dressing speed ratio (-)
Rz	Average surface roughness in μm
v_c	Cutting speed in m/s
v_{cd}	Cutting speed during dressing in m/s
v_{cs}	Cutting speed during sharpening in m/s
v_f	Feed rate in mm/min
v_{fd}	Feed rate during dressing in mm/min
v_{fs}	Feed rate during sharpening in mm/min
μ	Grinding force ratio (-)

References

1. Klocke, F. *Manufacturing Processes 2*; Springer: Berlin/Heidelberg, Germany, 2009.
2. Malkin, S.; Guo, C. *Grinding Technology: Theory and Applications of Machining with Abrasives*, 2nd ed.; Industrial Press: New York, NY, USA, 2008.
3. Kumar, S.; Paul, S. Numerical modelling of ground surface topography: Effect of traverse and helical superabrasive grinding with touch dressing. *Prod. Eng.* **2012**, *6*, 199–204. [CrossRef]
4. Teicher, U.; Künanz, K.; Ghosh, A.; Chattopadhyay, A.B. Performance of Diamond and CBN Single-Layered Grinding Wheels in Grinding Titanium. *Mater. Manuf. Process.* **2008**, *23*, 224–227. [CrossRef]
5. Kacalak, W.; Lipiński, D.; Bałasz, B.; Rypina, Ł.; Tandecka, K.; Szafraniec, F. Performance evaluation of the grinding wheel with aggregates of grains in grinding of Ti-6Al-4V titanium alloy. *Int. J. Adv. Manuf. Technol.* **2018**, *94*, 301–314. [CrossRef]
6. Nik, M.G.; Movahhedy, M.R.; Akbari, J. Ultrasonic-assisted grinding of Ti6Al4 V alloy. *Procedia Cirp* **2012**, *1*, 353–358. [CrossRef]
7. Rahman, M.; Wong, Y.S.; Zareena, A.R. Machinability of Titanium Alloys. *JSME Int. J. Ser C* **2003**, *46*, 107–115. [CrossRef]
8. Veiga, C.; Davim, J.; Loureiro, A. Properties and applications of titanium alloys: A brief review. *Rev. Adv. Mater. Sci.* **2012**, *32*, 133–148.

9. Guleryuz, H.; Cimenoglu, H. Oxidation of Ti–6Al–4V alloy. *J. Alloys Compd.* **2009**, *472*, 241–246. [CrossRef]
10. Zwicker, U. *Titan und Titanlegierungen*; Springer: Berlin/Heidelberg, Germany, 1974.
11. Agocs, A.; Besser, C.; Brenner, J.; Budnyk, S.; Frauscher, M.; Dörr, N. Engine oils in the field: A comprehensive tribological assessment of engine oil degradation in a passenger car. *Tribol. Lett.* **2022**, *70*, 28. [CrossRef]
12. Holländer, U.; Wulff, D.; Langohr, A.; Möhwald, K.; Maier, H.J. Brazing in SiH4-Doped Inert Gases: A New Approach to an Environment Friendly Production Process. *Int. J. Precis Eng. Manuf.-Green Tech.* **2019**, *7*, 1059–1071. [CrossRef]
13. Lützenkirchen-Hecht, D.; Wulff, D.; Wagner, R.; Frahm, R.; Holländer, U.; Maier, H.J. Thermal anti-oxidation treatment of CrNi-steels as studied by EXAFS in reflection mode: The influence of monosilane additions in the gas atmosphere of a continuous annealing furnace. *J. Mater. Sci.* **2014**, *49*, 5454–5461. [CrossRef]
14. Maier, H.J.; Herbst, S.; Denkena, B.; Dittrich, M.A.; Schaper, F.; Worpenberg, S.; Gustus, R.; Maus-Friedrichs, W. Towards Dry Machining of Titanium-Based Alloys: A New Approach Using an Oxygen-Free Environment. *Metals* **2020**, *10*, 1161. [CrossRef]
15. *ISO 3529-1:2019-07*; Vacuum Technology—Vocabulary—Part 1: General Terms. International Organization of Standardization: Geneva, Switzerland, 2019.
16. Friemuth, T. Schleifen Hartstoffverstärkter Keramischer Werkzeuge. Ph.D. Thesis, Universität Hannover, Hannover, Germany, 1999.
17. Kraus, W.; Nolze, G. POWDER CELL—A program for the representation and manipulation of crystal structures and calculation of the resulting X-ray powder patterns. *J. Appl. Crystallogr.* **1996**, *29*, 301–303. [CrossRef]
18. Ali, A.; Lockwood, F.; Klaus, E.E.; Duda, J.L.; Tewksbury, E.J. The chemical degradation of ester lubricants. *ASLE Trans.* **1979**, *22*, 267–276.
19. Clark, D.B.; Klaus, E.E. The role of iron and copper in the oxidation degradation of lubricating oils. *Lubr. Eng.* **1985**, *41*, 280–287.
20. Naidu, S.K.; Klaus, E.E.; Duda, J.L. Evaluation of liquid phase oxidation products of ester and mineral oil lubricant. *Ind. Eng. Chem. Prod. Res. Dev.* **1984**, *23*, 613–619.
21. Igasaki, Y.; Mitsuhashi, H. The effects of substrate bias on the structural and electrical properties of TiN films prepared by reactive r.f. sputtering. *Thin Solid Film.* **1980**, *70*, 17–25. [CrossRef]